

SLAC – PUB – 3541  
January 1985  
T/E

## MIXING OF TOPONIUM WITH THE $Z$ BOSON\*

PAULA J. FRANZINI AND FREDERICK J. GILMAN

*Stanford Linear Accelerator Center  
Stanford University, Stanford, California, 94305*

### ABSTRACT

We take seriously the possibility that toponium states are within several  $\text{GeV}/c^2$  of the  $Z$  boson mass and make a careful study of this possible near-degeneracy using the mass-mixing formalism. Most of the decay width of vector states below the open top threshold comes from mixing with the  $Z$ . In the idealized situation where there is no coupling of the unmixed toponium state to  $e^+e^-$  and  $f\bar{f}$ , the amplitude for  $e^+e^- \rightarrow f\bar{f}$  has an exact zero at the unmixed mass. Correspondingly, in the physical situation of non-zero couplings, the cross section for  $e^+e^- \rightarrow f\bar{f}$  exhibits deep minima. We investigate as well the effects of complex mixing matrix elements above the open top threshold, and calculate longitudinal polarization and forward-backward asymmetries, where there are large enhancements near toponium resonance masses.

Submitted to *Physical Review D*

---

\* Work supported by the Department of Energy, contract DE – AC03 – 76SF00515.

## 1. Introduction

The possibility of mixing between the  $Z^0$  boson and toponium ( $t\bar{t}$ ) states has already been discussed in a number of papers.<sup>1-4</sup> Much of this work, guided by theoretical speculation on the top quark mass,  $m_t$ , was concerned with the situation where the  $Z$  mass was much higher than  $2m_t$ . However the discovery of the  $Z^0$  at CERN,<sup>5</sup> and the more recent evidence<sup>6</sup> for a top quark with a mass between 30 GeV and 60 GeV suggests that the scenario where there is a near degeneracy in mass between toponium states and the  $Z$  merits a closer and more careful look.<sup>7</sup>

In the next section we set up the mass mixing formalism needed to study this problem. We then proceed to study the mixing of one vector ( $J^{PC} = 1^{--}$ ) toponium state,  $V$ , with the  $Z$ , solving the problem analytically and studying various limiting cases. There is an exact zero in the amplitude for  $e^+e^- \rightarrow f\bar{f}$  at the bare (unmixed) mass of the  $V$  when the couplings of the bare  $V$  state to both  $e^+e^-$  and  $f\bar{f}$  are zero. We set out the formulas for the couplings, cross sections, asymmetries, etc., and then consider the corrections of allowing non-zero couplings and of including  $e^+e^- \rightarrow \gamma \rightarrow f\bar{f}$ . For  $\sigma(e^+e^- \rightarrow f\bar{f})$  these have a small effect on the overall shape, which still has a strong minimum, whose position is slightly shifted. For the polarization and front-back asymmetries the effects are much more dramatic. The section concludes with the formalism needed for mixing the  $Z$  with an arbitrary number of vector toponium states, both below and above the open top threshold, where the off-diagonal mass mixing element becomes complex.

In section 3 we briefly discuss heavy quark potentials and the spectrum of toponium states which results. We use the potential of Richardson<sup>8</sup> and find

roughly 13 states below the open top threshold. Section 4 then contains the results following from applying the mixing formalism in Section 2 to the  $Z$  and the set of toponium states described in Section 3. We consider  $\sigma(e^+e^- \rightarrow f\bar{f})$  in situations where  $2m_t$  is less than, roughly equal to, and greater than  $M_Z$ . There are striking interference patterns observed in  $\sigma(e^+e^- \rightarrow f\bar{f})$  as well as in the longitudinal and front-back asymmetries. We conclude with a sobering look at what the experimentally unavoidable spread in beam energies does to these interference patterns.

## 2. Mixing

As we are considering mixing between states in a limited energy range far from threshold we may safely use the mass-mixing formalism.<sup>9,10</sup> If we take the simplified case of only two states, the  $Z$  and one vector ( $J^{PC} = 1^{--}$ ) toponium resonance,  $V$ , then the  $2 \times 2$  mass matrix has the form:

$$\mathcal{M}_0^2 = \begin{pmatrix} M_{V_0}^2 - i\Gamma_{V_0}M_{V_0} & \delta m^2 \\ \delta m^2 & M_{Z_0}^2 - i\Gamma_{Z_0}M_{Z_0} \end{pmatrix}, \quad (2.1)$$

and the matrix propagator,

$$\mathcal{D}(s) = \frac{1}{\mathcal{M}_0^2 - s\mathbf{1}}. \quad (2.2)$$

Here  $\mathcal{M}_0^2$  is the (undiagonalized) mass matrix with elements expressed in terms of “bare” masses ( $M_{Z_0}$  and  $M_{V_0}$ ) and widths ( $\Gamma_{Z_0}$  and  $\Gamma_{V_0}$ ). Within the spirit of the mass-mixing formalism we take the initial widths to be constants, with no explicit functional dependence on mass.<sup>9</sup> Inclusion of such a mass dependence, or working with the mass rather than mass-squared matrix, results in amplitude changes of a few percent in the limited mass range within which we are working.

The off diagonal term  $\delta m^2$ , which induces the mixing, originates in the (vector) coupling of the  $Z$  to the  $t$  quark contained in the toponium bound state (see Fig. 1). Its value is

$$\begin{aligned}\delta m^2 &= 2\sqrt{3} |\psi(0)| \sqrt{M_{V_0}} g_{v,t} \\ &= 2\sqrt{3} |\psi(0)| \sqrt{M_{V_0}} \left[ \frac{e(1 - \frac{8}{3} \sin^2 \theta_W)}{4 \sin \theta_W \cos \theta_W} \right],\end{aligned}\tag{2.3}$$

where  $\psi(0)$  is the wavefunction of the  $t\bar{t}$  bound state at the origin and  $\theta_W$  is the weak mixing angle (so that <sup>11</sup>  $\sin^2 \theta_W \approx 0.22$ ). The factor of  $\sqrt{3}$  arises from color. For the P states  $\delta m^2$  is proportional to the derivative of the wave function at the origin, with concomitant much smaller mixing (by roughly an order of magnitude for toponium). This is examined in detail in Ref. 7.

For purposes of calculation one can work with the mass matrix in this non-diagonal basis, sandwiching the propagator in Eq. (2.2) between initial and final spinors which express the coupling strength of the “bare”  $V_0$  and  $Z_0$  to the initial and final states respectively. For some purposes, however, it is more useful to go to the diagonal basis, obtaining along the way the physical states and eigenvalues. For this purpose we rewrite Eq. (2.1) as

$$\mathcal{M}_0^2 = \frac{1}{2} (M_{V_0}^2 - iM_{V_0}\Gamma_{V_0} + M_{Z_0}^2 - iM_{Z_0}\Gamma_{Z_0}) \mathbf{1} + \Delta^2 \hat{n} \cdot \vec{\sigma}\tag{2.4}$$

where

$$\Delta^2 = \sqrt{(M_{V_0}^2 - iM_{V_0}\Gamma_{V_0} - M_{Z_0}^2 + iM_{Z_0}\Gamma_{Z_0})^2/4 + (\delta m^2)^2},\tag{2.5a}$$

$$\hat{n} = \cos \theta \hat{z} + \sin \theta \hat{x}\tag{2.5b}$$

and the complex angle  $\theta$  is given by

$$\sin \theta = \delta m^2 / \Delta^2. \quad (2.5c)$$

It is then easy to see that  $\mathcal{R} M_0^2 \mathcal{R}^{-1}$ , where  $\mathcal{R} = e^{i\frac{\theta}{2}\sigma_y}$ , is diagonal, with eigenvalues

$$M_V^2 - iM_V\Gamma_V = \frac{1}{2}(M_{V_0}^2 - i\Gamma_{V_0}M_{V_0} + M_{Z_0}^2 - i\Gamma_{Z_0}M_{Z_0}) + \Delta^2 \quad (2.6a)$$

$$M_Z^2 - iM_Z\Gamma_Z = \frac{1}{2}(M_{V_0}^2 - i\Gamma_{V_0}M_{V_0} + M_{Z_0}^2 - i\Gamma_{Z_0}M_{Z_0}) - \Delta^2 \quad (2.6b)$$

and that the physical eigenstates are

$$\begin{aligned} |V\rangle &= e^{-i\frac{\theta}{2}\sigma_y} \begin{pmatrix} 1 \\ 0 \end{pmatrix} = \cos \frac{\theta}{2} |V_0\rangle - \sin \frac{\theta}{2} |Z_0\rangle \\ |Z\rangle &= e^{-i\frac{\theta}{2}\sigma_y} \begin{pmatrix} 0 \\ 1 \end{pmatrix} = \sin \frac{\theta}{2} |V_0\rangle + \cos \frac{\theta}{2} |Z_0\rangle. \end{aligned} \quad (2.7)$$

Since  $\theta$  is generally complex,  $\mathcal{R}$  is symmetric but not unitary.

When the narrow state  $V$  is far from the  $Z$ , these results simplify, and the mixing is characterized by

$$\frac{1}{2} \sin \theta \approx \frac{\theta}{2} \approx \frac{\delta m^2}{M_{V_0}^2 - M_{Z_0}^2 + iM_{Z_0}\Gamma_{Z_0}}. \quad (2.8)$$

As the magnitude of the right hand side turns out to be (see below)  $\lesssim 0.1$  even when  $M_{V_0} = M_{Z_0}$ , this is even a good approximation when the  $V$  and  $Z$  are close. The small admixture of the  $V_0$  in the  $Z$  has a totally negligible effect, while the corresponding small  $Z_0$  admixture to the  $V$  has relatively large effects because of the much larger  $Z_0$  couplings to fermion-antifermion pairs. Alternatively, when

the mixing is small, the problem of  $V$  decays involving the  $Z$  can be treated directly by explicitly calculating diagrams involving an intermediate  $Z$ , with identical results<sup>2</sup> to those obtained using Eq. (2.8).

Now let us consider the situation of interest to us when the state  $V_0$  is near the  $Z_0$  and most of the width of the  $V$  comes, as we shall see, from mixing with the  $Z$ . It is useful to consider then the idealized case where the unmixed state  $V_0$  has no coupling to particular initial and final states, *e.g.*,  $e^+e^-$  and  $\mu^+\mu^-$ . From Eq. (2.7) we see that in this case the couplings of the physical  $V$  and  $Z$  to the initial and final states are

$$\begin{aligned} g_v &= -\sin \frac{\theta}{2} g_{z_0} \\ g_z &= \cos \frac{\theta}{2} g_{z_0}. \end{aligned} \quad (2.9)$$

Consequently the scattering amplitude

$$A_{fi}(s) = \frac{g_{vf}g_{vi}}{M_V^2 - iM_V\Gamma_V - s} + \frac{g_{zf}g_{zi}}{M_Z^2 - iM_Z\Gamma_Z - s} \quad (2.10)$$

simplifies to

$$A_{fi}(s) = g_{z_0f}g_{z_0i} \left[ \frac{\sin^2 \frac{\theta}{2}}{M_V^2 - iM_V\Gamma_V - s} + \frac{\cos^2 \frac{\theta}{2}}{M_Z^2 - iM_Z\Gamma_Z - s} \right] \quad (2.11)$$

At the point  $s = M_{V_0}^2 - iM_{V_0}\Gamma_{V_0}$ , the (complex) mass squared of the unmixed toponium state,

$$A_{fi}(M_{V_0}^2 - iM_{V_0}\Gamma_{V_0}) = g_{z_0f}g_{z_0i} \left[ \frac{\sin^2 \frac{\theta}{2}}{\Delta^2(\cos \theta - 1)} + \frac{\cos^2 \frac{\theta}{2}}{\Delta^2(\cos \theta + 1)} \right] = 0 \quad (2.12)$$

when we use the relationship in Eqs. (2.6a,b) between the “dressed” masses and “bare” masses together with the definition of  $\theta$  in Eq. (2.5c). Therefore there

is an exact zero of the amplitude  $A_{fi}(s)$  at the position of the unmixed  $V_0$  mass when the unmixed state does not couple to either the initial or final state.<sup>12</sup>

How close is the actual situation to this idealized one? To answer this we need to put in some numerical values and insert couplings from the standard model. From the Richardson<sup>8</sup> potential discussed in the next section we take  $|\psi(0)|^2 \approx 65 \text{ GeV}^3$  for the 1S vector meson ground state of toponium when the top quark mass is such that its mass  $M_{V_0} \approx M_Z$  (which we take as<sup>11,13</sup> 93 GeV). According to Eq.(2.3), we then have

$$\delta m^2 = 20 \text{ GeV}^2 \quad (2.13)$$

for mixing of the 1S state with the  $Z_0$ .

Preservation of the trace of the mass matrix under diagonalization implies that  $M_V^2 - M_{V_0}^2 = -(M_Z^2 - M_{Z_0}^2)$ , so the squared masses are shifted equally and oppositely, and similarly for widths. We solve Eqs. (2.6) for the “dressed” masses and widths as a function of  $M_{V_0}$ , taking  $M_{Z_0}=93 \text{ GeV}$  and<sup>14</sup>  $\Gamma_{Z_0}=2.7 \text{ GeV}$  ( $\Gamma_{V_0} = \mathcal{O}(100 \text{ KeV})$  and can be neglected at this stage of the calculation), with the results shown in Figs. 2 and 3. The mass shift, at most about 4 MeV (i.e.  $\Delta M/M \lesssim 5 \times 10^{-5}$ ), is negligible. On the other hand  $V$  does acquire a sizable width which is maximal when the  $V_0$  and  $Z_0$  coincide, at which point

$$\Gamma_V \approx \frac{(\delta m^2)^2}{M_{Z_0}^2 \Gamma_{Z_0}} \approx 18 \text{ MeV}, \quad (2.14)$$

*i.e.*, more than two orders of magnitude greater than the bare width.

The calculation of the cross section, as well as the polarization and front-back asymmetries, is expedited by considering Feynman amplitudes  $A_{fi}$  for initial and

final fermions of definite handedness, which are in principle separately measurable and hence do not interfere (since the interactions are mixtures of V and A the corresponding antifermions are forced to have opposite handedness). The couplings of the gauge bosons to fermions of charge  $Qe$  and third component of weak isospin  $T_{3L}$  are given in the standard model as

$$\begin{aligned}
g_{z_0,L} &= e \frac{T_{3L} - Q \sin^2 \theta_W}{\sin \theta_W \cos \theta_W} \\
g_{z_0,R} &= e \frac{-Q \sin^2 \theta_W}{\sin \theta_W \cos \theta_W} \\
g_{\gamma,L} &= g_{\gamma,R} = eQ,
\end{aligned} \tag{2.15}$$

while that induced by an intermediate virtual photon for the  $V_0$  is

$$g_{v_0,L} = g_{v_0,R} = \frac{4}{3} e^2 Q \sqrt{3} (M_{V_0})^{-\frac{3}{2}} |\psi(0)|. \tag{2.16}$$

The angular dependence of the various amplitudes is given by standard arguments, so that the unpolarized cross section is

$$\begin{aligned}
\frac{d\sigma(s, \theta)}{d \cos \theta} &= \frac{s}{32\pi} \left[ |A_{L,L}(s)|^2 \left( \frac{1 + \cos \theta}{2} \right)^2 + |A_{L,R}(s)|^2 \left( \frac{1 - \cos \theta}{2} \right)^2 \right. \\
&\quad \left. + |A_{R,L}(s)|^2 \left( \frac{1 - \cos \theta}{2} \right)^2 + |A_{R,R}(s)|^2 \left( \frac{1 + \cos \theta}{2} \right)^2 \right].
\end{aligned} \tag{2.17}$$

Recalling  $\sigma_{pt}(s) = 4\pi\alpha^2/3s$ ,

$$R(s) = \frac{\sigma(s)}{\sigma_{pt}(s)} = \frac{s^2}{64\pi^2\alpha^2} [|A_{L,L}(s)|^2 + |A_{L,R}(s)|^2 + |A_{R,L}(s)|^2 + |A_{R,R}(s)|^2]. \tag{2.18}$$

The value of  $R$  for  $e^+e^- \rightarrow \mu^+\mu^-$  in the situation where  $M_{V_0}$  is 1 GeV below  $M_Z$ , which we arbitrarily choose for the purposes of illustration, is shown in Fig.



4. The dotted curve is with the  $Z$  alone, while the dashed line shows the case in which the couplings of the  $V_0$  to initial and final fermions are set to zero. We find in this latter case that

$$R = \frac{(|g_{Z_0,L}|^2 + |g_{Z_0,R}|^2)(|g_{Z_0,L}|^2 + |g_{Z_0,R}|^2)_f}{64\pi^2\alpha^2} \times \left| \frac{s(s - M_{V_0}^2 + i\Gamma_{V_0}M_{V_0})}{(s - M_{V_0}^2 + i\Gamma_{V_0}M_{V_0})(s - M_{Z_0}^2 + i\Gamma_{Z_0}M_{Z_0}) - (\delta m^2)^2} \right|^2. \quad (2.19)$$

Here we have done the calculation in the unmixed basis, where it is easier. As demanded by Eq. (2.12), there is an exact zero of the amplitude at a value of  $s$  equal to the (complex) bare mass squared of the  $V_0$ . While not visible in Fig. 4, the dashed curve does not precisely go through zero, but to  $R \approx 5 \times 10^{-3}$ , since we have made  $\Gamma_{V_0} = 100$  KeV and the zero of the amplitude is slightly off the real energy axis. The realistic case, including the photon intermediate state and bare  $V_0$  couplings as per Eq. (2.16), is shown by the solid line. There still is a deep dip near  $M_{V_0}$ . A similar dip occurs for all the  $^3S_1$  states below open top threshold, except that the effect occurs over a narrower energy region for the higher states since their widths (acquired mostly from mixing) are smaller. When  $M_{V_0} > M_{Z_0}$  the dip occurs before the peak, rather than after it as in Fig. 4. For the very fortuitous case where  $M_{V_0} = M_{Z_0}$ , there is no peak at all; only a near zero right in the middle of the  $Z$ . Similar behavior is exhibited for  $e^+e^- \rightarrow u\bar{u}$  and  $e^+e^- \rightarrow d\bar{d}$ .

Since we have the cross section in terms of amplitudes for fermions of definite handedness it is easy to find the expression for the longitudinal polarization (of

the initial  $e^-$  asymmetry:

$$A_{pol}(s, \theta) = \frac{A_1(s) + \frac{2 \cos \theta}{1 + \cos^2 \theta} A_2(s)}{1 + \frac{2 \cos \theta}{1 + \cos^2 \theta} A_{FB}(s)} \quad (2.20)$$

where

$$A_1 = \frac{|A_{R,R}|^2 + |A_{L,R}|^2 - |A_{R,L}|^2 - |A_{L,L}|^2}{|A_{R,R}|^2 + |A_{L,R}|^2 + |A_{R,L}|^2 + |A_{L,L}|^2} \quad (2.21)$$

$$A_2 = \frac{|A_{R,R}|^2 + |A_{R,L}|^2 - |A_{L,R}|^2 - |A_{L,L}|^2}{|A_{R,R}|^2 + |A_{L,R}|^2 + |A_{R,L}|^2 + |A_{L,L}|^2}$$

and the front-back asymmetry

$$A_{FB} = \frac{|A_{R,R}|^2 + |A_{L,L}|^2 - |A_{L,R}|^2 - |A_{R,L}|^2}{|A_{R,R}|^2 + |A_{L,R}|^2 + |A_{R,L}|^2 + |A_{L,L}|^2}. \quad (2.22)$$

(The quantity  $A_{FB}$  used here has a maximum magnitude of unity. The more usual front-back asymmetry obtained by integrating over the forward and backward hemispheres, is a factor of 3/4 smaller.) If we pay no attention to the angular distribution of the final state fermions and integrate over the center-of-mass scattering angle  $\theta$ , then we are only sensitive to  $A_1(s)$ , which is sometimes referred to as “the” polarization asymmetry. For  $e^+e^- \rightarrow \mu^+\mu^-$ ,  $A_1(s) = A_2(s)$  and there is no distinction between them anyway. Fig. 5 displays the polarization asymmetry for the reaction  $e^+e^- \rightarrow \mu^+\mu^-$  when  $M_{V_0}$  is 1 GeV less than  $M_{Z_0}$ . Again the dashed line gives the result when the bare  $V_0$  has no coupling to the initial or final fermions. Since in this case the coupling of the  $V$  to the initial and final fermions comes entirely through mixing with the  $Z_0$ , the ratios of its helicity couplings are identical to those of the  $Z$  and the value of  $A_{pol}$  is identical to that for the  $Z$  alone. However, when the amplitudes involving virtual photons are included (solid line in Fig. 5), the effects are dramatic. Although the amplitudes

involving virtual photons are small, those coming from  $V + Z$  also are small near  $M_{V_0}$  and one sees a large effect characteristic of the interference of the real part of the Breit-Wigner of the  $V$  with the rest of the amplitude.

Fig. 6 shows the polarization asymmetries  $A_1$  and  $A_2$  in the vicinity of  $M_{V_0}$  for production of charge  $\frac{2e}{3}$  and  $-\frac{e}{3}$  quarks,  $u$  and  $d$ . Again one observes characteristic interference patterns due to the real part (e.g., in  $A_1$  for  $u\bar{u}$ ) and/or imaginary part (e.g., in  $A_2$  for  $d\bar{d}$ ) of the Breit-Wigner resonance amplitude of the  $V$  interfering with the rest of the amplitude due to  $\gamma + Z$ . The quark production amplitudes used in this computation do not include the contributions from strong interactions, *i.e.*,  $V \rightarrow$  intermediate gluons  $\rightarrow q\bar{q}$ , which could in principle contribute further coherently interfering amplitudes, modifying the interference patterns. Similar comments hold for the forward-backward asymmetry shown in Fig. 7 for  $\sqrt{s}$  in the neighborhood of  $M_{V_0}$ . As the asymmetries for  $\gamma + Z$  alone do not vary strongly over the width of the  $Z$ , the general form of the asymmetry after the state  $V$  is introduced does not depend strongly on whether it is a few GeV below or above the  $Z$  mass.

The extension of the formalism to encompass mixing of the  $Z$  with an arbitrary number of toponium states is straightforward. For  $n$  states the mass matrix is  $(n+1) \times (n+1)$ :

$$\mathcal{M}_0^2 = \begin{pmatrix} M_{Z_0}^2 - iM_{Z_0}\Gamma_{Z_0} & \delta m^2 & \delta m'^2 & \dots \\ \delta m^2 & M_{V_0}^2 - iM_{V_0}\Gamma_{V_0} & 0 & 0 \\ \delta m'^2 & 0 & M_{V'_0}^2 - iM_{V'_0}\Gamma_{V'_0} & 0 \\ \vdots & 0 & 0 & \ddots \end{pmatrix} \quad (2.23)$$

where  $\delta m^2$ ,  $\delta m'^2$ ,  $\dots$  parametrize the mixing between the  $Z$  and the spectrum

of toponium states  $V, V', \dots$ . Mixing directly (e.g, through an intermediate photon) between toponium states is very small and has been neglected.

If one works only to second order in  $\delta m^2, \delta m'^2, \dots$  then it is possible to write a simple expression for the rotation that diagonalizes  $M_0^2$  and hence its eigenvalues and eigenvectors. We have found numerically that this gives a fair approximation to the masses and widths of the dressed states  $V, V', \dots$ , and a good approximation to the cross sections. In our subsequent work we calculate in the unmixed basis, as the matrix can be inverted exactly. While this can be done analytically, it is easier to carry out the matrix manipulations numerically at each value of  $s$ .

Finally, above open top threshold two interesting effects occur. The bare width of the toponium states will no longer be negligible, changing the near zeroes in cross sections to minima where the cross section drops by less than an order of magnitude. Further, the mixing term  $\delta m^2$  picks up an imaginary part as physical intermediate states are allowed ( $V_0 \rightarrow T_i \bar{T}_i \rightarrow Z_0$ ), giving

$$\text{Im}\delta m^2 = - \sum_i \sqrt{M_{Z_0} \Gamma_{Z_0 \rightarrow T_i \bar{T}_i}} \sqrt{M_{V_0} \Gamma_{V_0 \rightarrow T_i \bar{T}_i}}, \quad (2.24)$$

where the sum extends over all physical intermediate states. In principle the imaginary part of  $\delta m^2$  can be comparable to the real part, causing sizable changes in the interference.

### 3. Toponium States and Thresholds

We shall be utilizing the spectrum of toponium states and their wave functions determined using the heavy quark potential of Richardson.<sup>8</sup> It has the advantages of correct long and short range behavior together with a minimal number of parameters. In addition it provides a very good set of predictions for the  $^3S_1$  states of the upsilon system.<sup>15</sup> This potential is specified in momentum space by:

$$\tilde{V}(q^2) = -\frac{4}{3} \frac{12\pi}{33 - 2n_f} \frac{1}{q^2 \ln(1 + q^2/\Lambda^2)}. \quad (3.1)$$

It can be rewritten in position space as:

$$V(r) = \frac{8\pi}{33 - 2n_f} \Lambda \left( \Lambda r - \frac{f(\Lambda r)}{\Lambda r} \right), \quad (3.2)$$

where

$$f(t) = \left[ 1 - 4 \int_1^\infty \frac{dq}{q} \frac{e^{-qt}}{[\ln(q^2 - 1)]^2 + \pi^2} \right]. \quad (3.3)$$

We evaluate this potential numerically using<sup>8</sup>  $\Lambda = .398\text{GeV}$ , and then solve the radial Schrödinger equation,

$$u'' + \frac{2(l+1)}{r} u' + \frac{2\mu}{\hbar^2} [E - V(r)] u = 0, \quad (3.4)$$

where  $l$  is the angular momentum and  $u(r) \cdot r^l = R(r)$ , the radial wavefunction. The first several energy levels, as a function of the top quark mass,  $m_t$ , are shown in Fig. 8. The corresponding values of  $\psi(0) = R(0)/\sqrt{4\pi}$ , the wavefunction at the

origin for the S states, are shown in Fig. 9. These wavefunctions are normalized with the condition

$$4\pi \int |\psi(r)|^2 r^2 dr = 1. \quad (3.5)$$

With this normalization the leptonic width (through an intermediate photon) is<sup>16,17</sup>

$$\Gamma(V_0 \rightarrow e^+e^-) = \frac{16\pi\alpha^2}{M_{V_0}^2} |\psi(0)|^2 Q_t^2, \quad (3.6)$$

and corresponds to a leptonic width of about 9 KeV for the ground state.

To calculate where the threshold for bare top production occurs, we basically follow Eichten and Gottfried.<sup>18</sup> If we use the charm quark as a baseline we have

$$m_T - m_t = m_D - m_c + \frac{3}{4}(1 - m_c/m_t)\delta_c, \quad (3.7)$$

where the last term corrects for the hyperfine splitting between the  $D^*$  and  $D$  and between the  $T^*$  and  $T$  (the quantity  $\delta_c = m_{D^*} - m_D = .141$  GeV). Inserting the mass of the charm quark appropriate to the Richardson potential (1.491 GeV), and the experimental D mass, yields  $m_T - m_t = 0.477$  GeV. Alternately, we may use the bottom system as a baseline:

$$m_T - m_t = m_B - m_b + \frac{3}{4}(1 - m_b/m_t)\delta_b, \quad (3.8)$$

where now<sup>19</sup>  $\delta_b = m_{B^*} - m_B = .052$  GeV. Again, inserting the quark mass appropriate to the Richardson potential ( $m_b = 4.883$  GeV), we find  $m_T - m_t = 0.425$  GeV.

The threshold is found at  $2m_T$ , i.e.,  $.95 \text{ GeV} + 2m_t$  or  $.85 \text{ GeV} + 2m_t$  from Eq. (3.7) or Eq. (3.8), respectively. In Fig. 8 we have taken it to be at  $.95 \text{ GeV} + 2m_t$  (indicated by the solid line), with the result that there are 13  $^3S_1$  states below open top threshold for  $m_t \approx 45 \text{ GeV}$ . Since the level spacing is about one  $^3S_1$  state per hundred MeV near threshold, we would lose one such state to the continuum if we moved the threshold down to  $2m_t + 0.85 \text{ GeV}$ .

#### 4. Cross Sections and Asymmetries for Toponium Near the $Z$

We are now in a position to put together the mixing formalism in Section 2 with the toponium spectrum and functions of Section 3. Indeed, for the ground state of toponium we have already done this in that we explored the consequences of the mixing formalism by using it as an example in Section 2 for mass shifts, cross sections, and asymmetries in the two state system consisting of the  $1S$  state,  $V_0$ , and the  $Z_0$ . Figures 10, 11, and 12 show the cross section in the neighborhood of the  $Z$ , for  $e^+e^- \rightarrow \mu^+\mu^-$ , normalized to  $\sigma_{pt} = 4\pi\alpha^2/3s$ , for situations where  $m_t=45, 47, \text{ and } 49 \text{ GeV}$  respectively. In each case the distinct interference pattern of each of the thirteen  $^3S_1$  states assumed to be below open top threshold is visible. As we move over the peak of the  $Z$  the peak-dip order in the interference changes to dip-peak.

The width (acquired by mixing) of the toponium states decreases as we go to higher energy levels because the wave function at the origin (see Fig. 9) decreases, and so proportionally does the amplitude for mixing with the  $Z$ . However, the height of the peak (in R) remains approximately the same. This is exactly correct

for a resonance,  $V$ , which acquires all its width from mixing with the  $Z$ , for

$$\sigma_{\text{peak},V}(e^+e^- \rightarrow \mu^+\mu^-) \propto \frac{1}{M_V^2} \left( \frac{\Gamma_{e,V}^{1/2}\Gamma_{\mu,V}^{1/2}}{\Gamma_{\text{total},V}} \right)^2 \quad (4.1)$$

and therefore

$$R_{\text{peak},V}(e^+e^- \rightarrow \mu^+\mu^-) \propto \left( \frac{\Gamma_{e,V}^{1/2}\Gamma_{\mu,V}^{1/2}}{\Gamma_{\text{total},V}} \right)^2 \quad (4.2)$$

where the constant of proportionality involves dimensionless couplings, numbers, etc. But for a state whose width comes entirely from mixing with the  $Z$ , the ratio of widths on the right hand side of Eq. (4.1) or Eq. (4.2) is the same as for the  $Z$ , and thus  $R_{\text{peak},V}(e^+e^- \rightarrow \mu^+\mu^-) = R_{\text{peak},Z}(e^+e^- \rightarrow \mu^+\mu^-)$ , independent of  $M_V$ . The slight rise in  $R_{\text{peak},V}$  in Figs. 10, 11 and 12 as we move from resonance to resonance is caused by using the mass mixing formalism with  $\Gamma_{Z_0}$  fixed to calculate  $\Gamma_{\text{total},V}$ , but keeping (implicitly) the mass dependence in  $\Gamma_{e,V}$  and  $\Gamma_{\mu,V}$ .

Once we are above open top threshold, the situation changes considerably. The width of an unmixed toponium state presumably becomes tens of MeV, as is the case for the  $\Psi''$  and  $\Upsilon'''$ . The peak and dip structure from interference with the  $Z$  is much less dramatic in  $e^+e^- \rightarrow \mu^+\mu^-$ , as is shown in Fig. 13. Here we have illustrated the situation by taking the  $14^3S_1$  state to be 2 GeV above the  $Z$  and to have a width of 20 MeV for decay into pairs of open top states. The dashed line shows the case of real  $\delta m^2$  while the solid line indicates what happens when there is an imaginary part of the same magnitude (but opposite sign), which is a plausible possibility from Eq. (2.23). The imaginary part of  $\delta m^2$  makes the interference pattern somewhat more impressive but when we note the suppressed zero for the vertical axis in Fig. 13 it is clear that in any case for



$e^+e^- \rightarrow \mu^+\mu^-$  we have a much less impressive effect than that for a resonance below threshold. Of course, if we look at  $e^+e^- \rightarrow t\bar{t}$ , we will see a much greater effect, for  $t\bar{t}$  is the major decay of such a resonance while  $\mu^+\mu^-$  is a very minor one. However, once we are above open top threshold the situation becomes quite complicated in that different states will mix with each other as well as the  $Z$  and the approximation inherent in producing zeroes in the mass matrix in Eq. (2.23) breaks down. At the same time all the mixing matrix elements become complex. While interesting, a detailed investigation is beyond the scope of this paper.

The situation with respect to the polarization or front-back asymmetries when we include the whole spectrum of  $^3S_1$  toponium states is very much an iteration of what is found in Figs. 5, 6, and 7 for the 1S state. Of course, there are small variations as the  $t$  quark mass is changed and the “background” asymmetries due to the  $\gamma$  and  $Z$  change, but the general form of the interference pattern remains the same as we move over the peak of the  $Z$ . Again as we go to higher radial excitations, the width of the mixed toponium states decreases (to  $\lesssim 1$  MeV just below threshold) making the measurement of these large swings in the asymmetries very difficult.

This brings us to the question of how much of this is in fact measurable under actual experimental conditions where the spread in beam energy is not negligible. To see how this affects the results we have taken the curve in Fig. 11 (corresponding to  $m_t=47$  GeV), which would be the measured cross section with no beam energy spread, and smeared it with a Gaussian corresponding to  $\sigma_{E_{\text{beam}}} = 40$  MeV (*i.e.*,  $\sigma_E/E \approx 0.8 \times 10^{-3}$ ) and to  $\sigma_{E_{\text{beam}}} = 100$  MeV (*i.e.*,  $\sigma_E/E \approx 2 \times 10^{-3}$ ). The result is shown by the solid and dashed line respectively, in Fig. 14. The latter case is presently the specification for the SLC, although the

former case, which is roughly nominal LEP performance without wigglers, is also achievable<sup>20</sup> at SLC. In the latter case the structure due to the higher  $^3S_1$  states is washed out and we can only see a mild undulation due to the  $1S$  state, instead of the deep dip in Fig. 4. In the former case, with a narrower beam spread, the ground state is quite clear and a few higher states can be picked off from their interference pattern with the  $Z$ .

The effects of smearing with  $\sigma_{E_{b.e.m.}}=40$  MeV on  $A_{pol}$  and  $A_{FB}$  are shown for the ground state of toponium in Figs. 15 and 16, respectively. Part of the reason these asymmetries have such a small variation when  $M_{V_0}$  is near  $M_Z$  (e.g.  $M_{V_0}=92$  GeV in the figures), is that the unpolarized cross section due to the  $Z$  (which occurs in the denominator of the expression for the asymmetries) is large there. Even with the smearing one has fairly sizable effects in the asymmetries well below<sup>21</sup> or well above the  $Z$ .

Thus with  $\sigma_{E_{b.e.m.}} \approx 40$  MeV one should be able to see quite distinctive indications for the first few levels of toponium both in the cross section and the polarization and front-back asymmetries. Even with  $\sigma_{E_{b.e.m.}} \approx 100$  MeV, if Nature is kind enough to put toponium near the  $Z$ , the effects due to interference of the ground state with the  $Z$  are visible, and they are capable at least of giving us information on the properties of the  $t$  quark and in particular, fairly precise knowledge of  $m_t$  and hence of where to look for open top threshold.

## Acknowledgements

We thank M. Peskin for suggestions and for the use of his program implementing the Richardson potential, and S. Güsken, H. Kühn and P. Zerwas for communicating the results of their work before publication, as well as P. Zerwas for several discussions. One of us (P.J.F) would also like to thank B. Ratra and J. Yeager for helpful suggestions.

## REFERENCES

1. F. M. Renard, *Z. Phys.* **C1**, 225 (1979).
2. L. M. Sehgal and P. M. Zerwas, *Nucl. Phys.* **B183**, 417 (1981). See also R. Budny, *Phys. Rev.* **D20**, 2763 (1979), and J. D. Jackson, S.L. Olsen, and S.H.H. Tye, in *Proceedings of the 1982 Summer Study on Elementary Particles and Fields, Snowmass*, edited by R. Donaldson, R. Gustafson, and F. Paige (Amer. Inst. Phys., N.Y., 1983), p.175. L. M. Chang and J. N. Ng, TRIUMF preprint (1984) (unpublished).
3. I. I. Y. Bigi and H. Krasemann, *Z. Phys* **C7**, 127 (1981); J. H. Kühn, in *Proceedings of the 1982 Schladming School (Electroweak Interactions), Schladming*, edited by H. Mitter (Springer-Verlag, Vienna, 1982), p.203; L. M. Sehgal, in *Proceedings of the 1983 Europhysics Study Conf. on Electroweak Effects at High Energies, Erice*, edited by H. D. Newman (Plenum, New York, 1985), (to be published); J. H. Kühn and S. Ono, *Z. Phys.* **C21**, 395 (1984).
4. E. Eichten, in *Proceedings of the 1984 SLAC Summer Institute on Particle Physics, Stanford*, edited by P. McDonough (Stanford Linear Accel. Center, Stanford, 1985), (to be published).
5. G. Arnison *et. al.*, *Phys. Lett.* **126B**, 398 (1983) and **135B**, 250 (1984); P. Bagnaia *et. al.*, *Phys. Lett.* **129B**, 130 (1983).
6. G. Arnison *et. al.*, *Phys. Lett.* **147B** 493 (1984).
7. S. Güsken, J. H. Kühn, and P. M. Zerwas, paper in preparation. See also J. H. Kühn, and P. M. Zerwas, CERN preprint TH.4089/85 (1985) (unpublished).

8. J. L. Richardson, Phys. Lett. **82B**, 272 (1979).
9. S. Coleman and H.J. Schnitzer, Phys. Rev. **134**, 863 (1964).
10. F. M. Renard, Springer Tracts in Mod. Phys. **63**, 98 (1972); Y. Dothan and D. Horn, Nucl. Phys. **B114**, 400 (1976).
11. Particle Data Group, Rev. Mod. Phys. **56**, No. 2, Part II, S296 (1984).
12. We thank M. Peskin for pointing out to us an explanation for the vanishing amplitude by noting that in the unmixed basis  $M_0^2 - s\mathbf{1}$  has a zero for its  $V_0 - V_0$  element and consequently  $(M_0^2 - s\mathbf{1})^{-1}$  has a zero for its  $Z_0 - Z_0$  element at  $s = M_{V_0}^2 - iM_{V_0}\Gamma_{V_0}$ . It is this latter matrix element that is picked off when the inverse propagator is sandwiched between coupling spinors when the  $V_0$  has no coupling to either the initial or final fermions.
13. We take  $M_Z=93$  GeV for the remainder of the paper. All other masses are given relative to it, so that as a more exact value of the  $Z$  mass is measured, all our curves can be shifted appropriately.
14. With three generations of both quarks and leptons, but no contribution of the top quark to the  $Z$  width,  $\Gamma_Z=2.7$  GeV including  $\mathcal{O}(\alpha_s)$  corrections. The  $t$  and  $\bar{t}$  quarks in the  $^3S_1$  toponium states have a total width of  $\approx 70$  KeV to decay weakly for  $m_t=45$  GeV, which is comparable to, or greater than, the combined width for such a state to decay by annihilation through photons or gluons, or to decay by a transition to another toponium state. Hence we take  $\Gamma_{V_0} = 100$  KeV for illustrative purpose.
15. K. Gottfried, in *Proceedings of the 1981 International School of Nuclear Physics, Erice*, edited by D. Wilkinson (Pergamon Press, Oxford, 1982), p. 49. See also K. Gottfried, in *Proceedings of the Int. Europhysics Conf. on*

*High Energy Physics (Proceedings of HEP83), Brighton*, edited by J. Guy and C. Costain (Rutherford Lab., Chilton, 1983), p. 747.

16. R. Van Royen and V. Weisskopf, *Nuovo Cimento*, **50**, 617 (1967).
17. We have omitted QCD radiative corrections to  $\Gamma_{ee}$ ; these would decrease the width by a factor of about 0.8.
18. E. Eichten and K. Gottfried, *Phys. Lett.* **66B**, 286 (1977). See also C. Quigg and J. L. Rosner, *Phys. Lett.* **72B**, 462 (1978).
19. J. Lee-Franzini, in *Proceedings of the 22nd Int. Conf. on High Energy Physics, Leipzig, 1984*, (Akademie der Wissenschaften der DDR, Zeuth, 1985), (to be published). See also K. Han et. al., *Phys. Rev. Lett.* (to be published) (1985).
20. R. Stiening, private communication.
21. We thank P. Zerwas for pointing out the still sizable effects in asymmetries left after smearing when toponium is well below the  $Z$ . See Ref. 7 for a detailed discussion.

## FIGURE CAPTIONS

1. Diagrammatic representation of the process causing  $Z_0$ — $V_0$  mixing.
2. Change in the mass of the physical  $Z$  state due to mixing with the ground state of toponium as a function of the mass difference of the bare states ( $M_{Z_0}$  is held fixed at 93 GeV, while  $M_{V_0}$  is varied).
3. Change in the width of the physical ground state of toponium,  $V$ , as a function of the mass difference of the bare states ( $M_{Z_0}$  is held fixed at 93 GeV, while  $M_{V_0}$  is varied).
4.  $R(e^+e^- \rightarrow \mu^+\mu^-)$  arising through the  $Z$  alone (dotted line), through  $Z$  and  $V$  but no coupling of  $V_0$  to the initial or final states (dashed line), and from  $Z$ ,  $V$ , and  $\gamma$  including bare  $V_0$  couplings (solid line). The  $V_0$ -state has a total width of 100 KeV, and mass of 92 GeV.
5. a,b Polarization asymmetry with the toponium ground state 1 GeV/ $c^2$  below the  $Z$  ( $M_{V_0}=92$  GeV/ $c^2$ ). The polarization asymmetry is shown with all effects considered (solid line), and additionally in the more detailed figure,  $A_{pol}$  for the  $Z$  alone is shown (dashed line).
6. a,b The two polarization asymmetry components,  $A_1$  and  $A_2$ , for  $e^+e^- \rightarrow u\bar{u}$  and  $e^+e^- \rightarrow d\bar{d}$  in the vicinity of the ground state of toponium when  $M_{V_0}=92$  GeV/ $c^2$ .
7. The forward-backward asymmetry for  $e^+e^- \rightarrow \mu^+\mu^-$ ,  $e^+e^- \rightarrow u\bar{u}$  and  $e^+e^- \rightarrow d\bar{d}$  in the vicinity of the ground state of toponium when  $M_{V_0}=92$  GeV/ $c^2$ .
8. Binding energy of the  $S$  and  $P$  states of toponium, versus  $m_t$ , where  $m(tt) = 2m_t + E_B$ . The heavy line at 0.95 GeV is the threshold for open top

production relative to  $2m_t$ , which has a very weak dependence on  $m_t$ , for such large values of  $m_t$  (see text).

9. Wavefunction at the origin, from the Richardson potential, for the  $S$  states of toponium, versus  $m_t$ .
10.  $R(e^+e^- \rightarrow \mu^+\mu^-)$ , including mixing of the  $Z$  with the first thirteen toponium states, for  $m_t = 45$  GeV.
11.  $R(e^+e^- \rightarrow \mu^+\mu^-)$ , including mixing of the  $Z$  with the first thirteen toponium states, for  $m_t = 47$  GeV.
12.  $R(e^+e^- \rightarrow \mu^+\mu^-)$  including mixing of the  $Z$  with the first thirteen toponium states, for  $m_t = 49$  GeV.
13.  $R(e^+e^- \rightarrow \mu^+\mu^-)$  for a 14S state of toponium with  $M_{V_0}=95$  GeV/ $c^2$  and  $\Gamma_{V_0}=20$  MeV, and real  $\delta m^2$  (dashed curve), and complex  $\delta m^2$  with  $\text{Im}\delta m^2/\text{Re}\delta m^2 = -1$  (solid curve). The dotted curve is for the  $Z$  alone.
14. The curve in Figure 11, convoluted with a gaussian appropriate for  $\sigma_{\text{beam}}=40$  MeV (solid line) and  $\sigma_{\text{beam}}=100$  MeV (dashed line). We show  $R(e^+e^- \rightarrow \mu^+\mu^-)$  due to the  $Z$  alone (dotted line) for comparison.
15. The polarization asymmetry near the 1S state of toponium for  $\sigma_{\text{beam}}=40$  MeV when  $M_{V_0}=84, 92,$  and  $100$  GeV.
16. The front-back asymmetry near the 1S state of toponium for  $\sigma_{\text{beam}}=40$  MeV when  $M_{V_0}=84, 92,$  and  $100$  GeV.



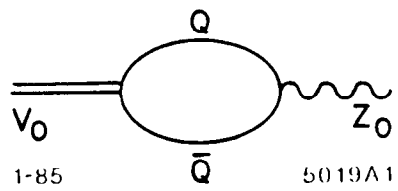
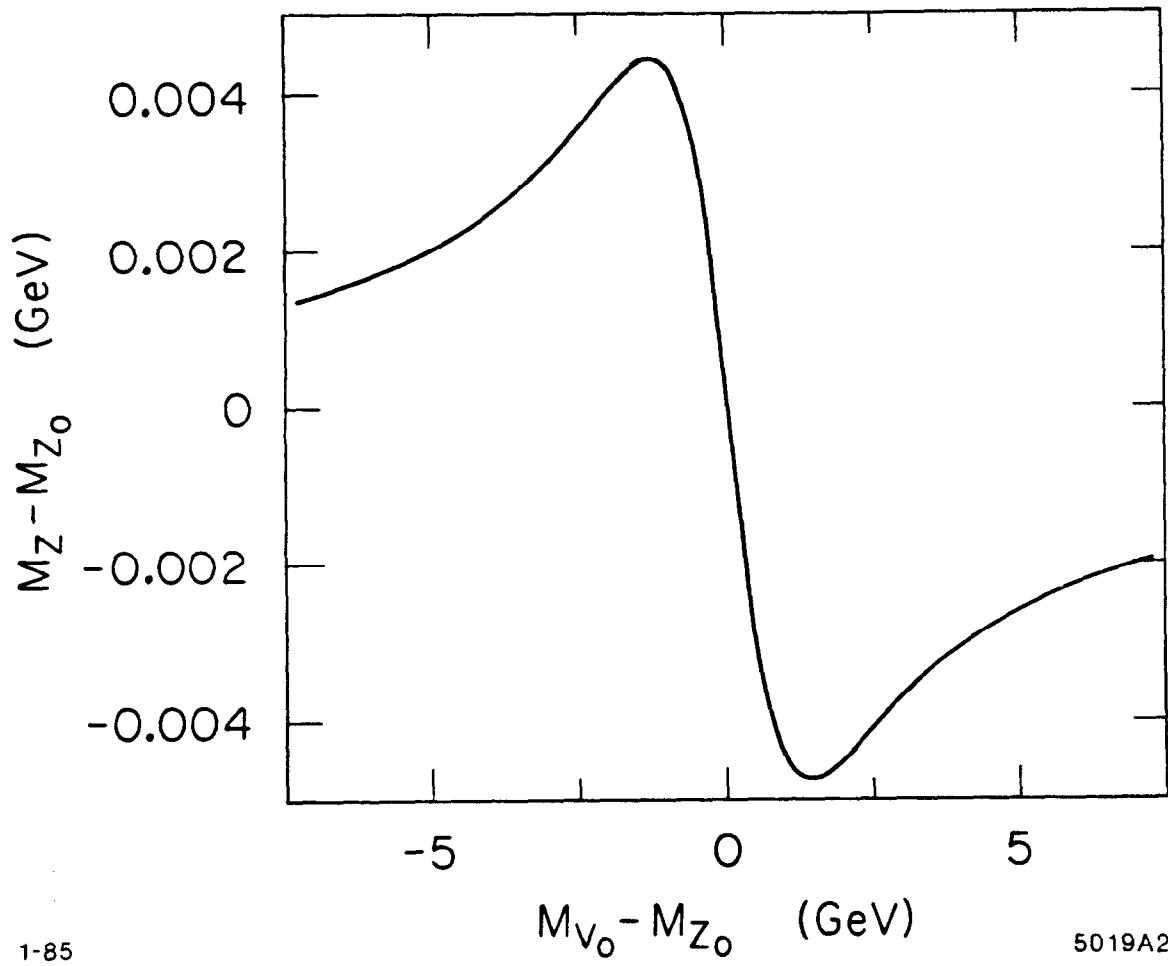


Fig. 1



1-85

5019A2

Fig. 2

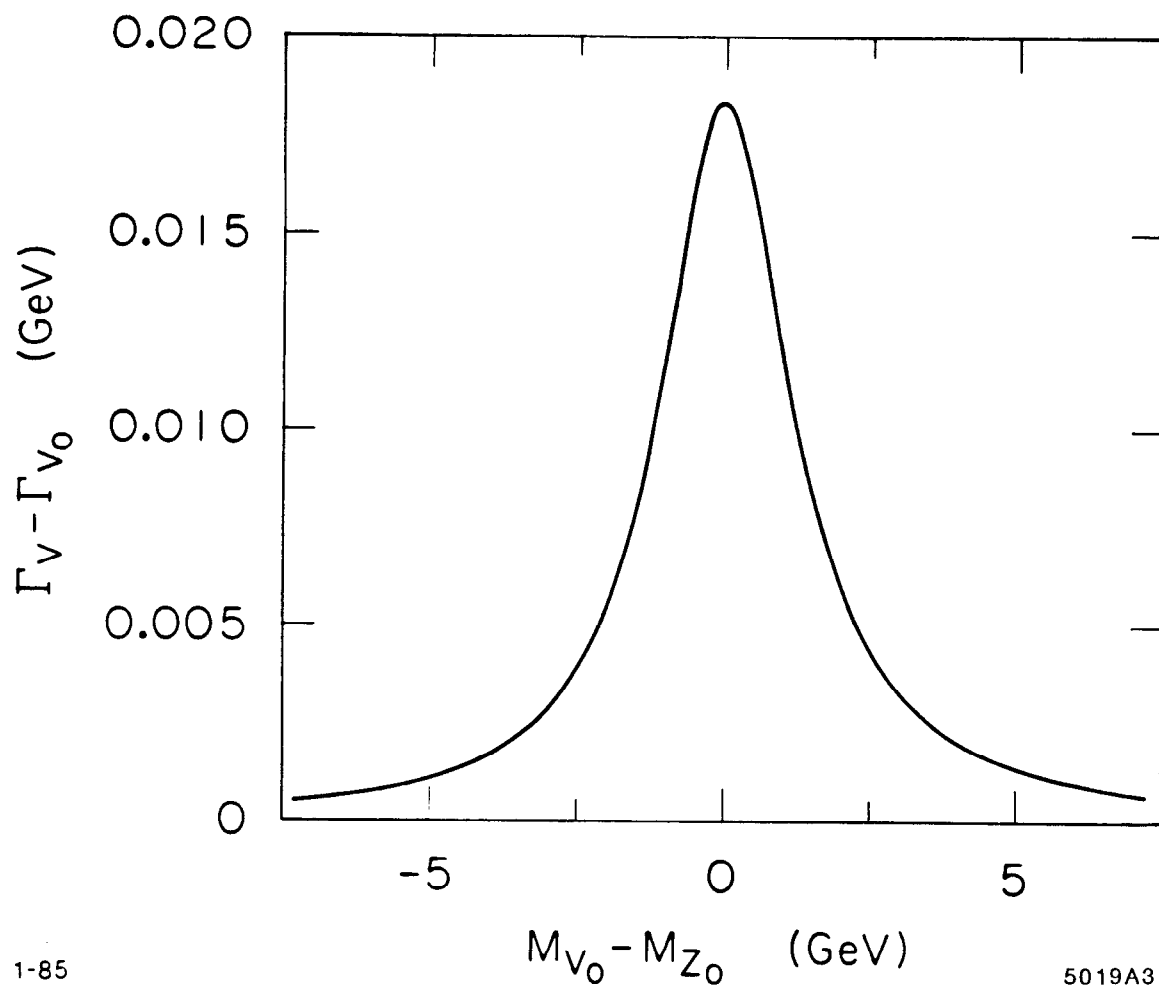
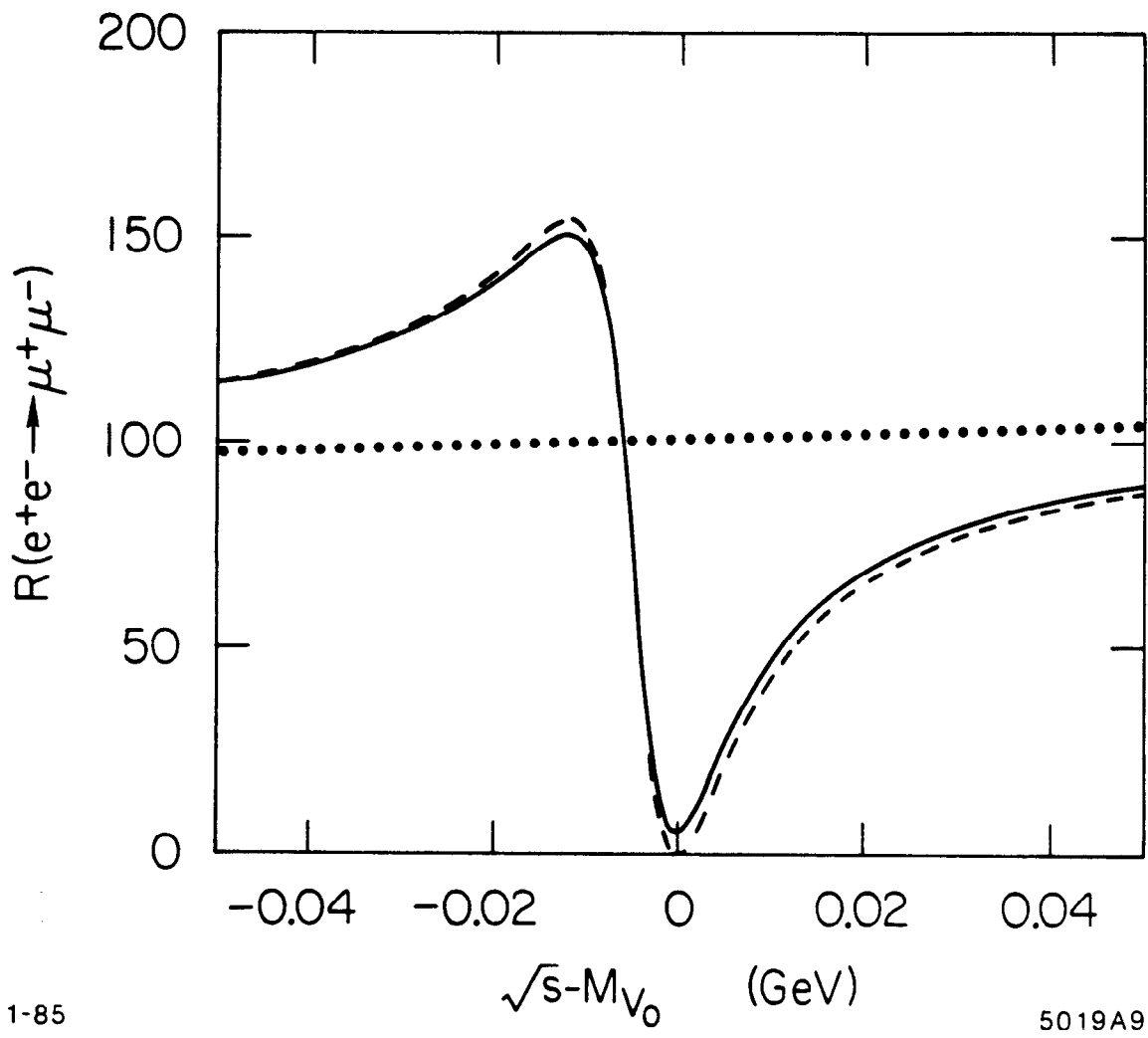


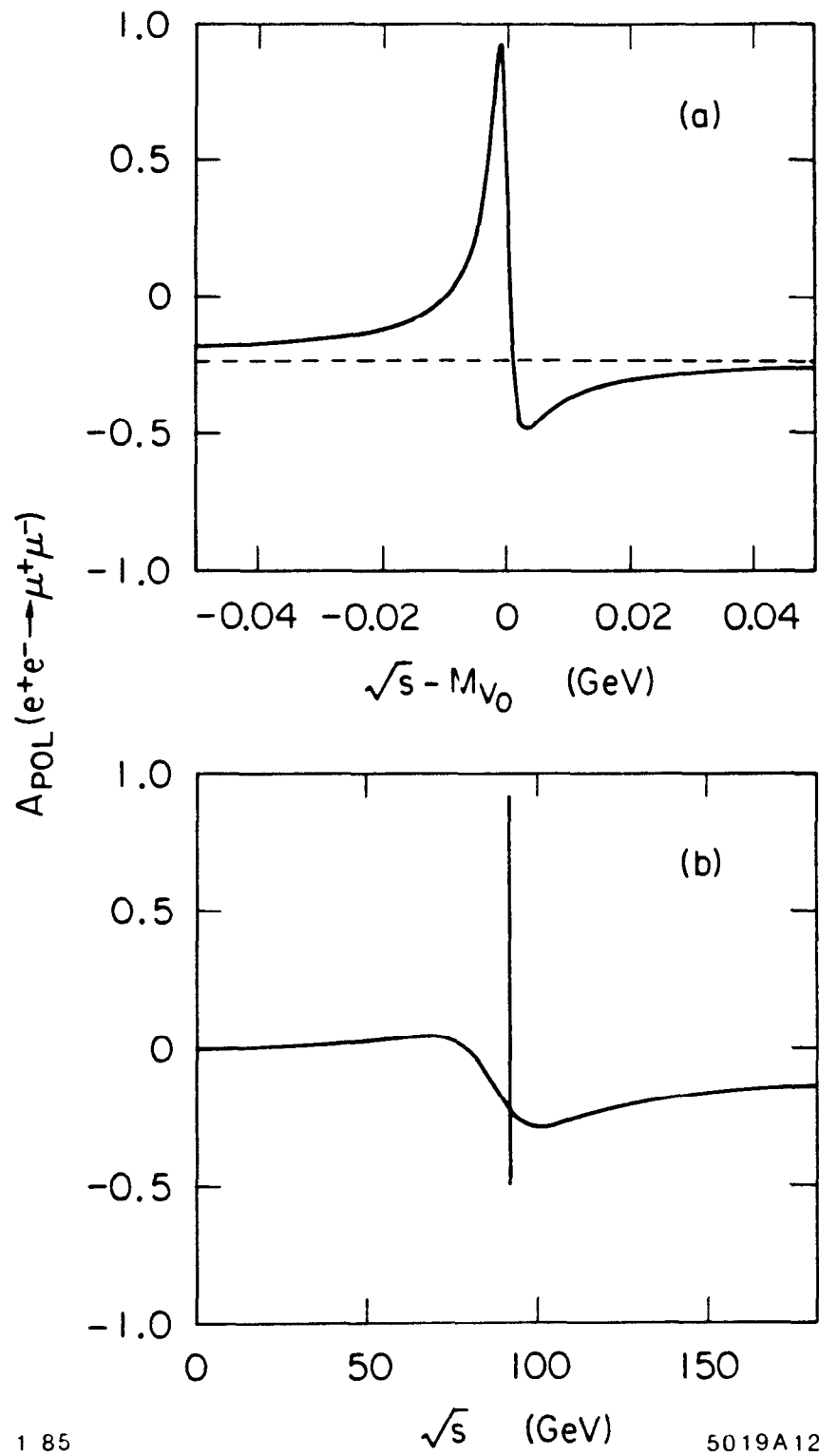
Fig. 3



1-85

5019A9

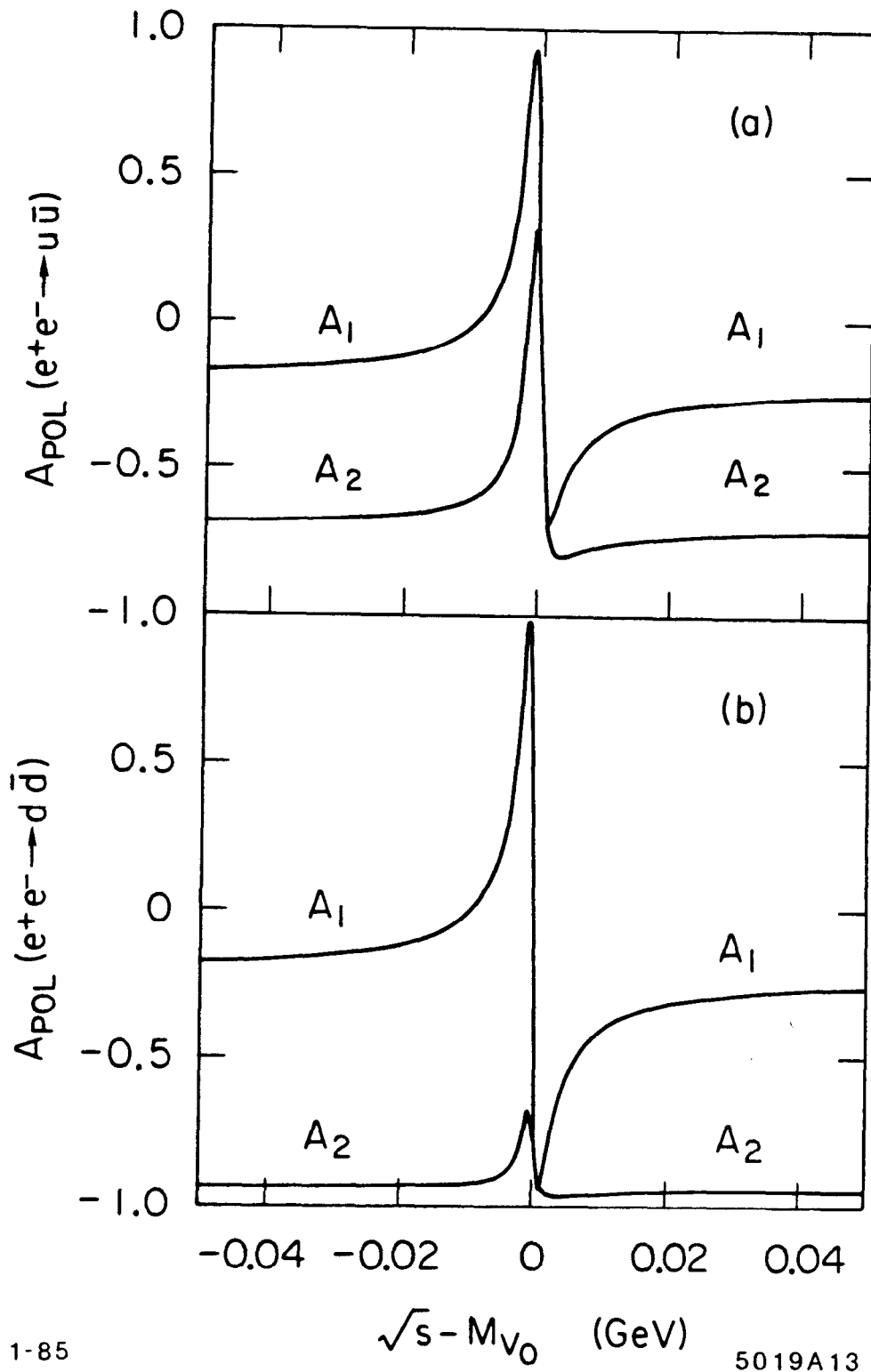
Fig. 4



1 85

5019A12

Fig. 5



1-85

5019A13

Fig. 6

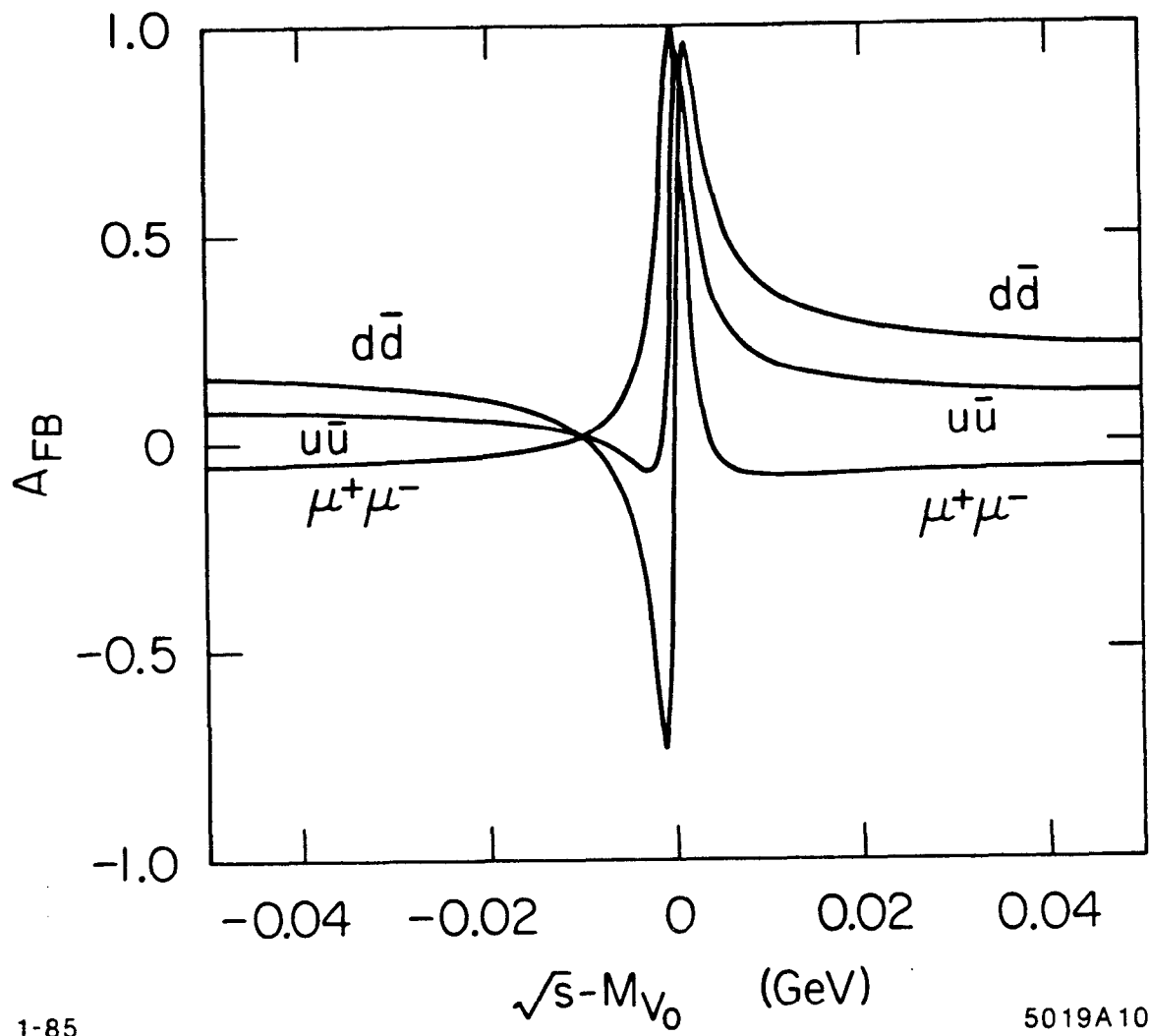
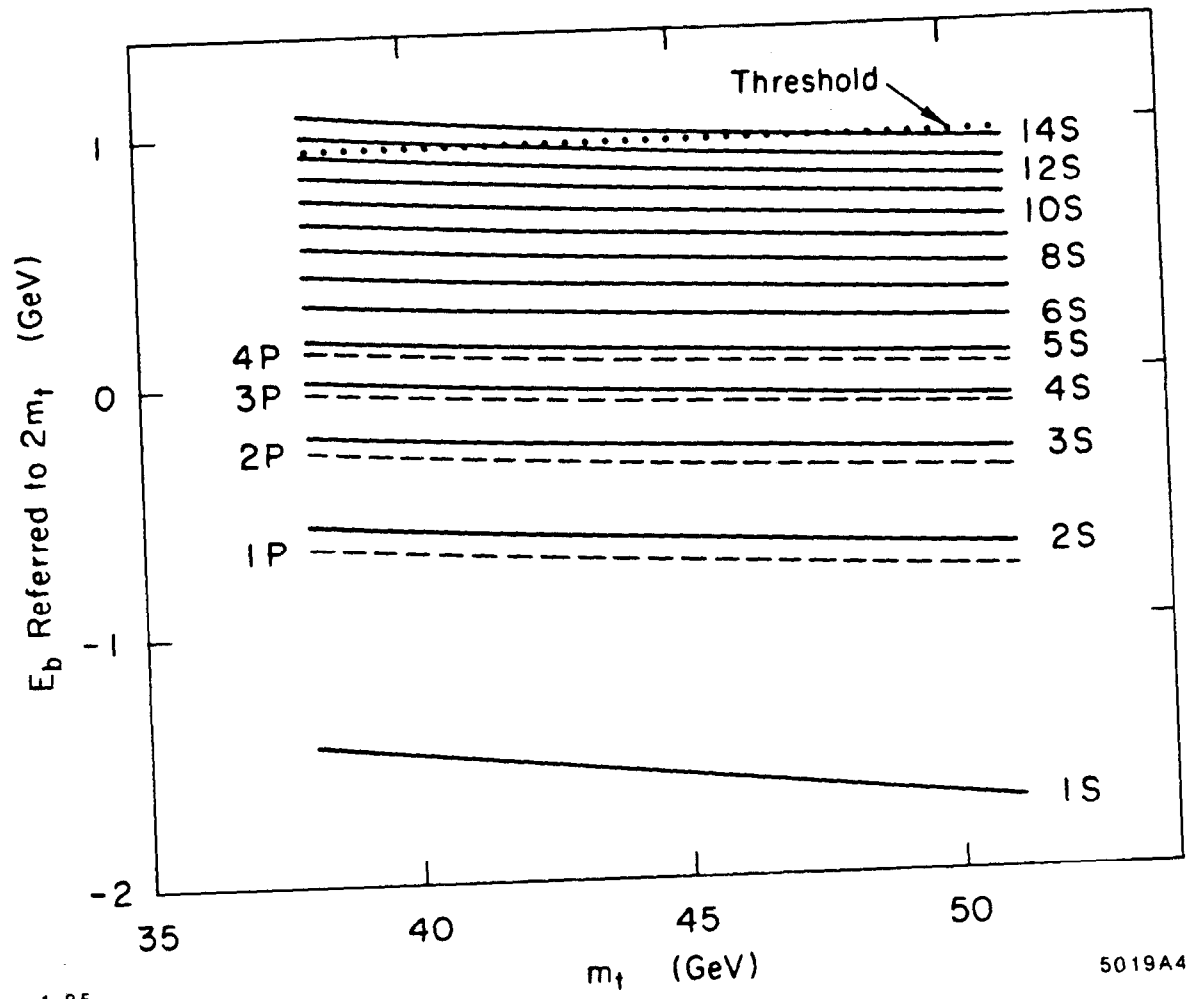


Fig. 7



1-85

5019A4

Fig. 8



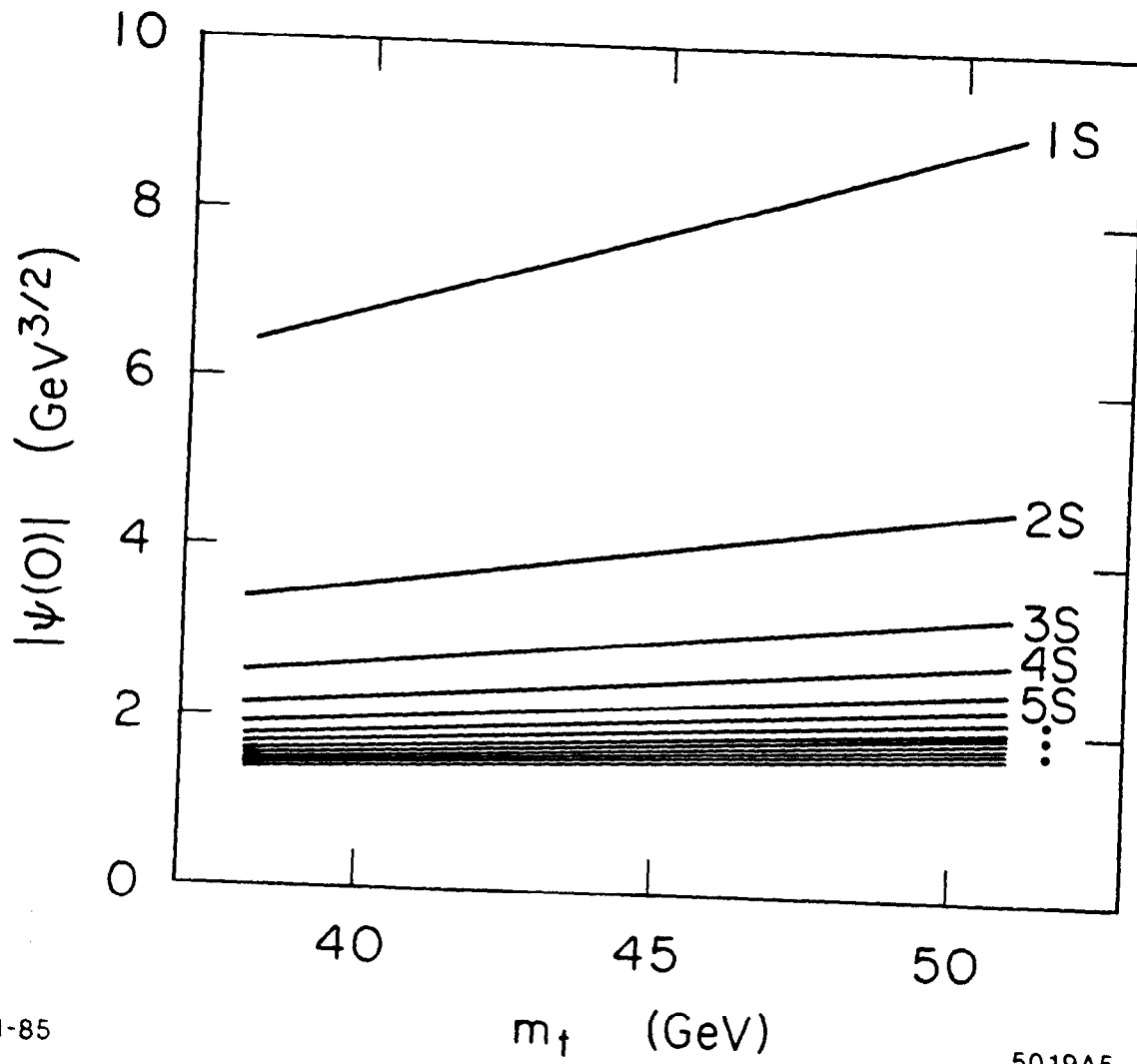


Fig. 9

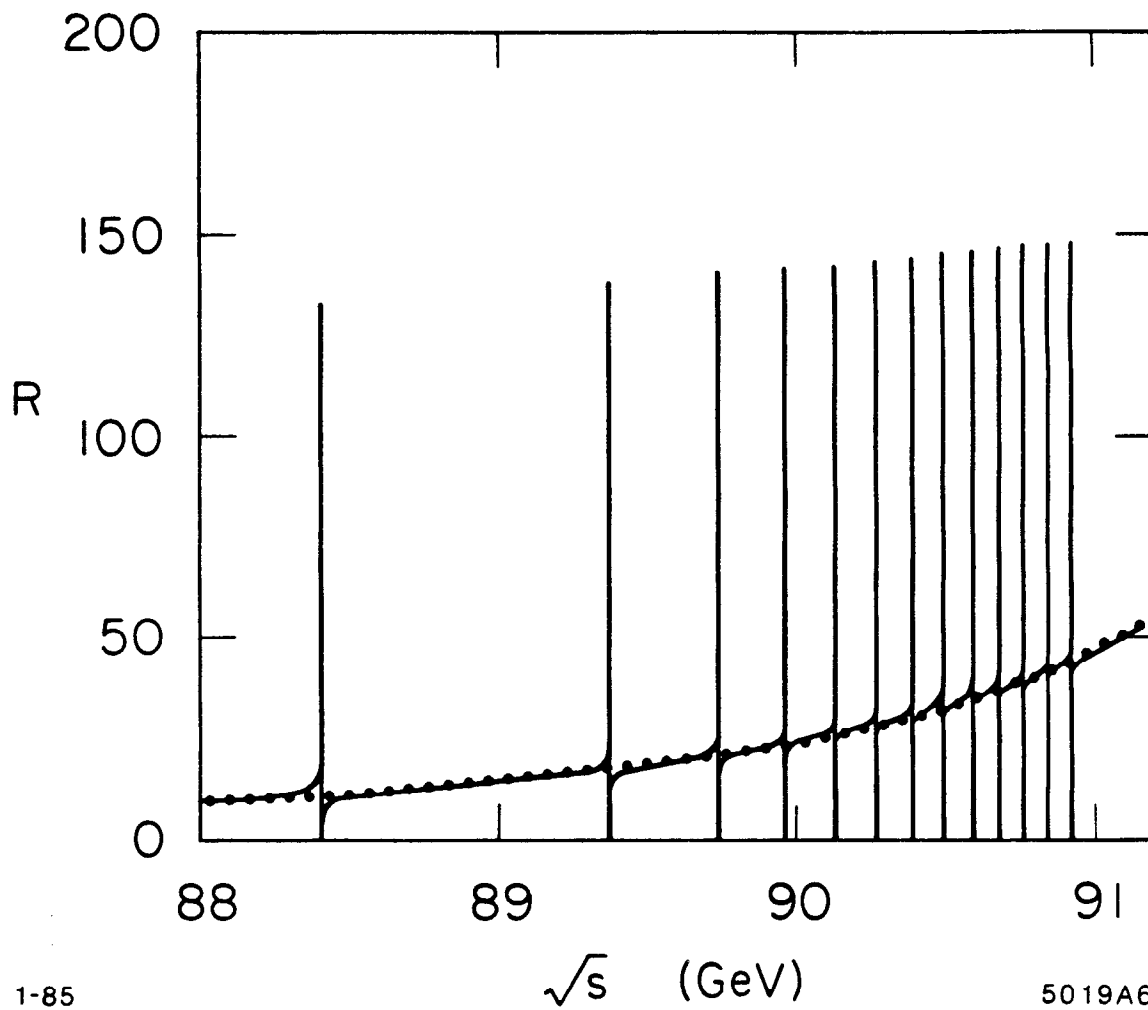
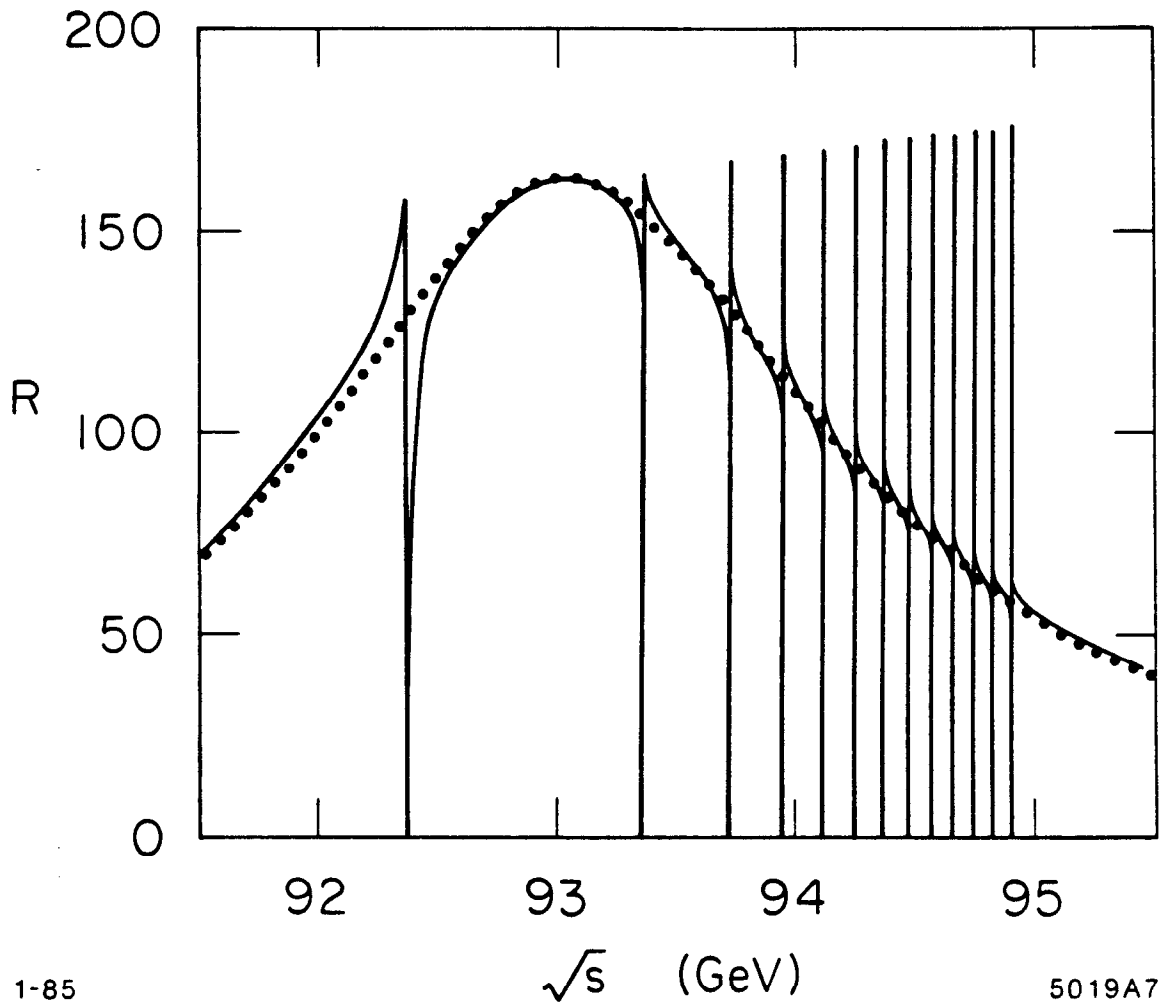


Fig. 10



1-85

$\sqrt{s}$  (GeV)

5019A7

Fig. 11

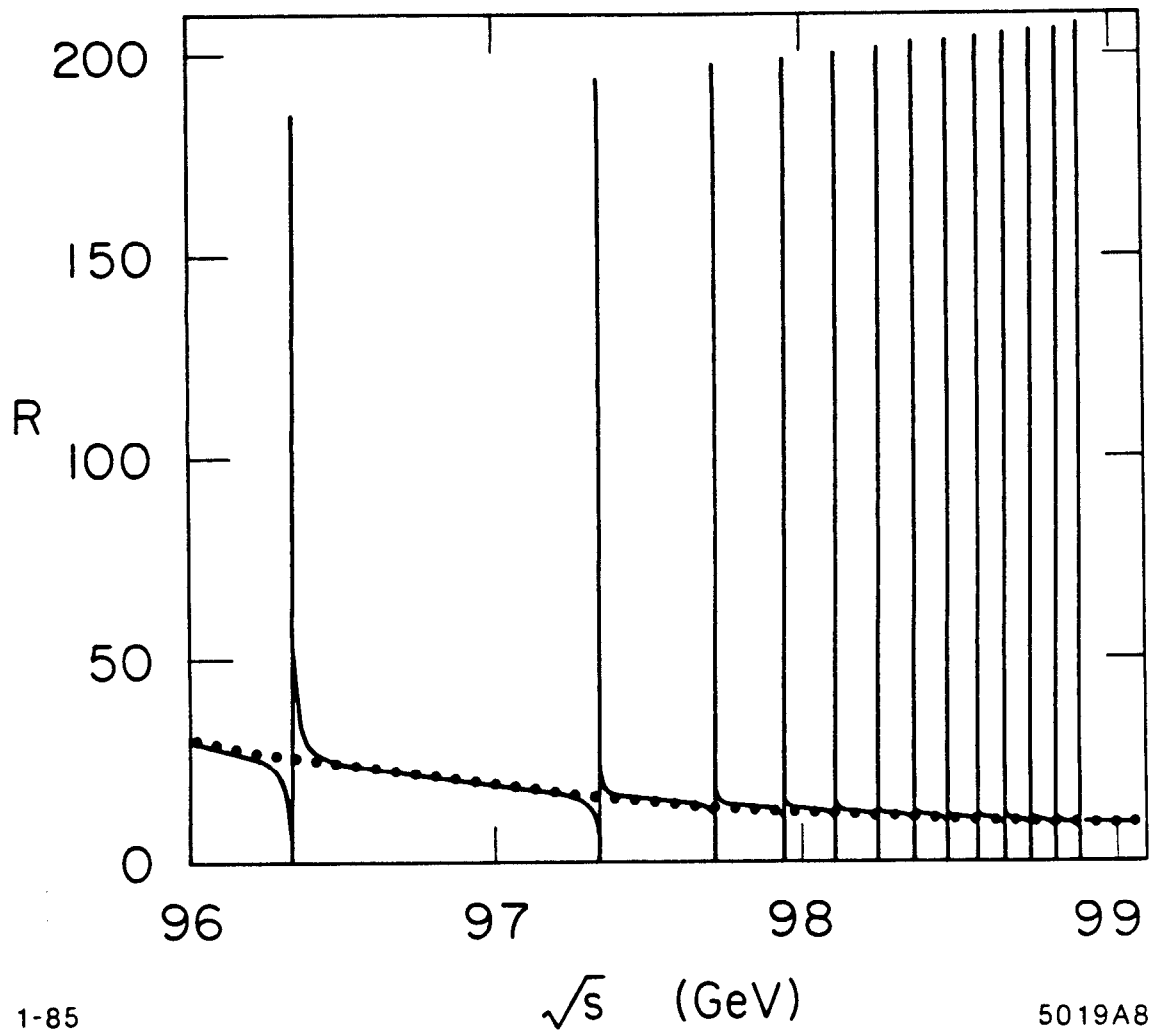
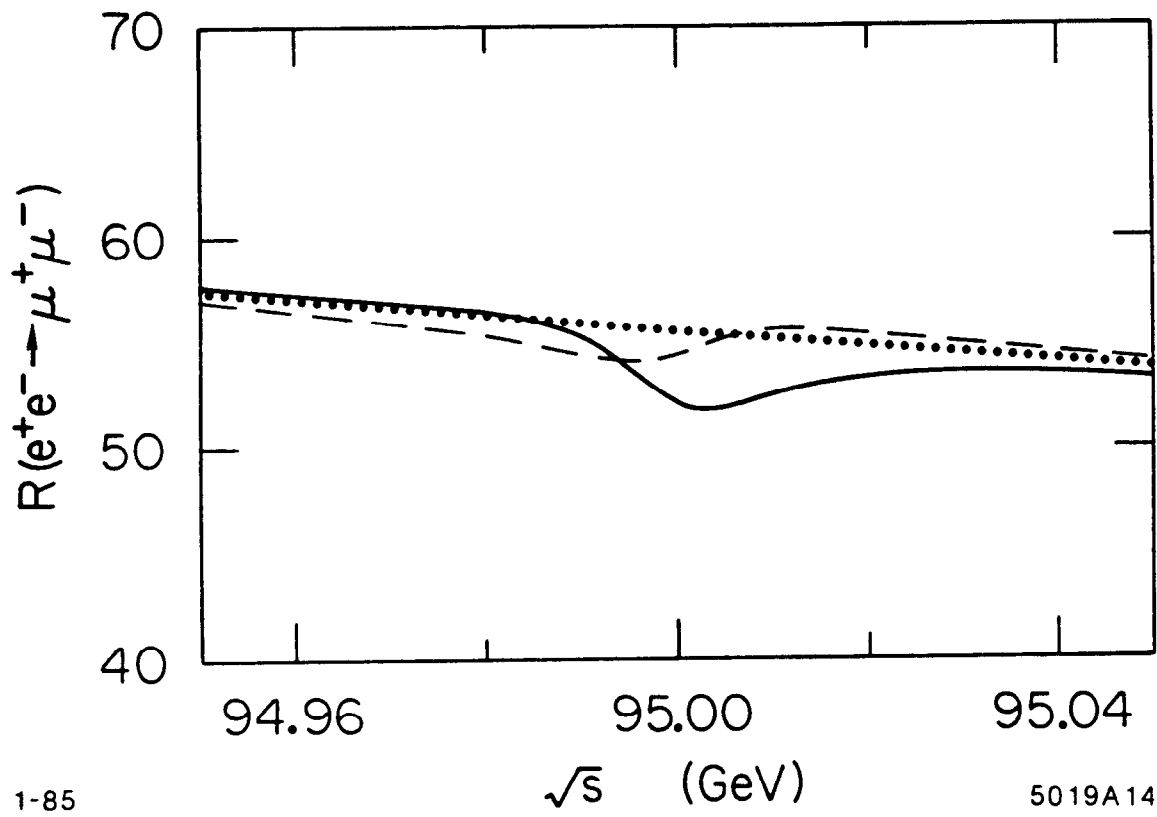


Fig. 12

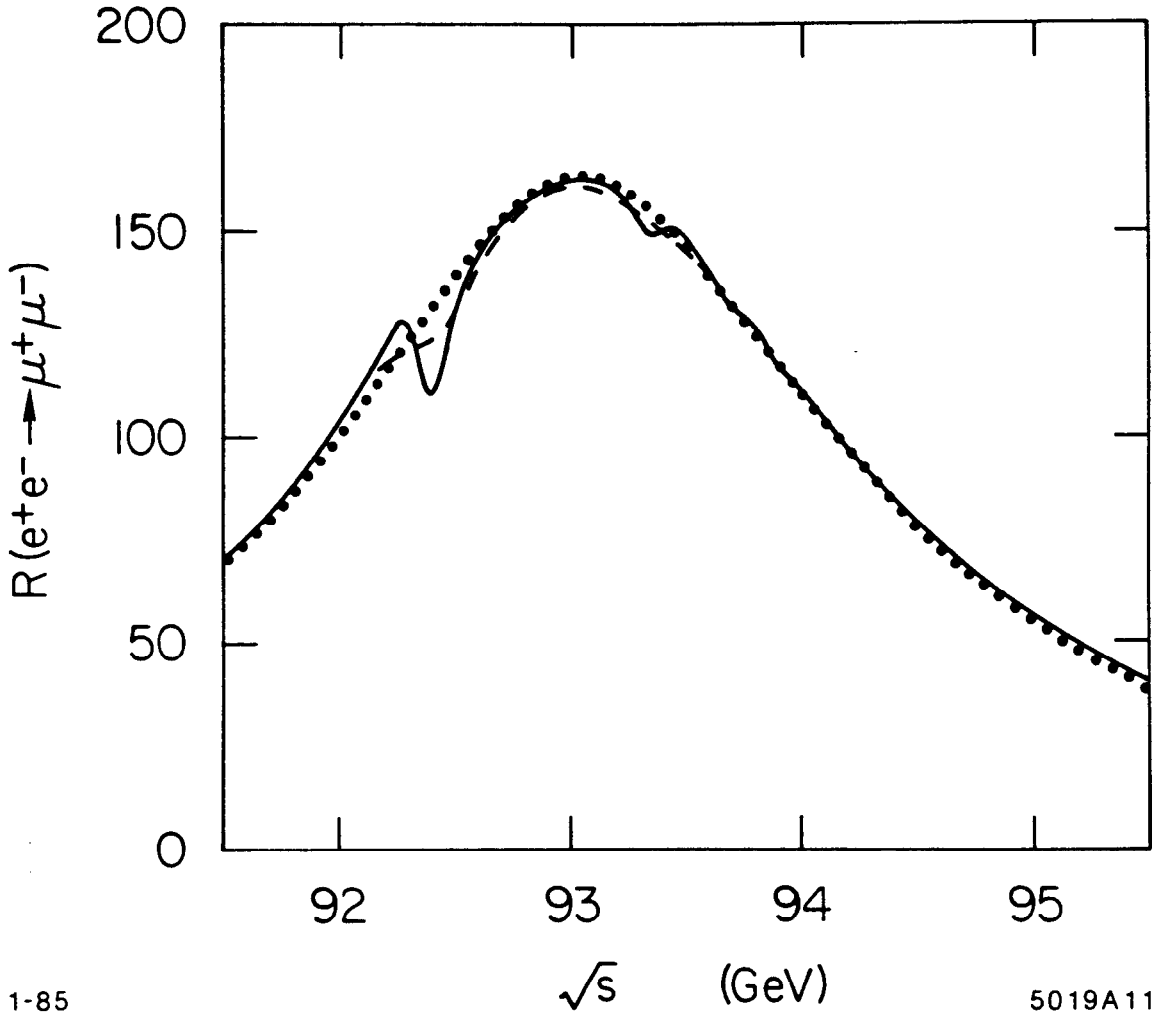


1-85

$\sqrt{s}$  (GeV)

5019A14

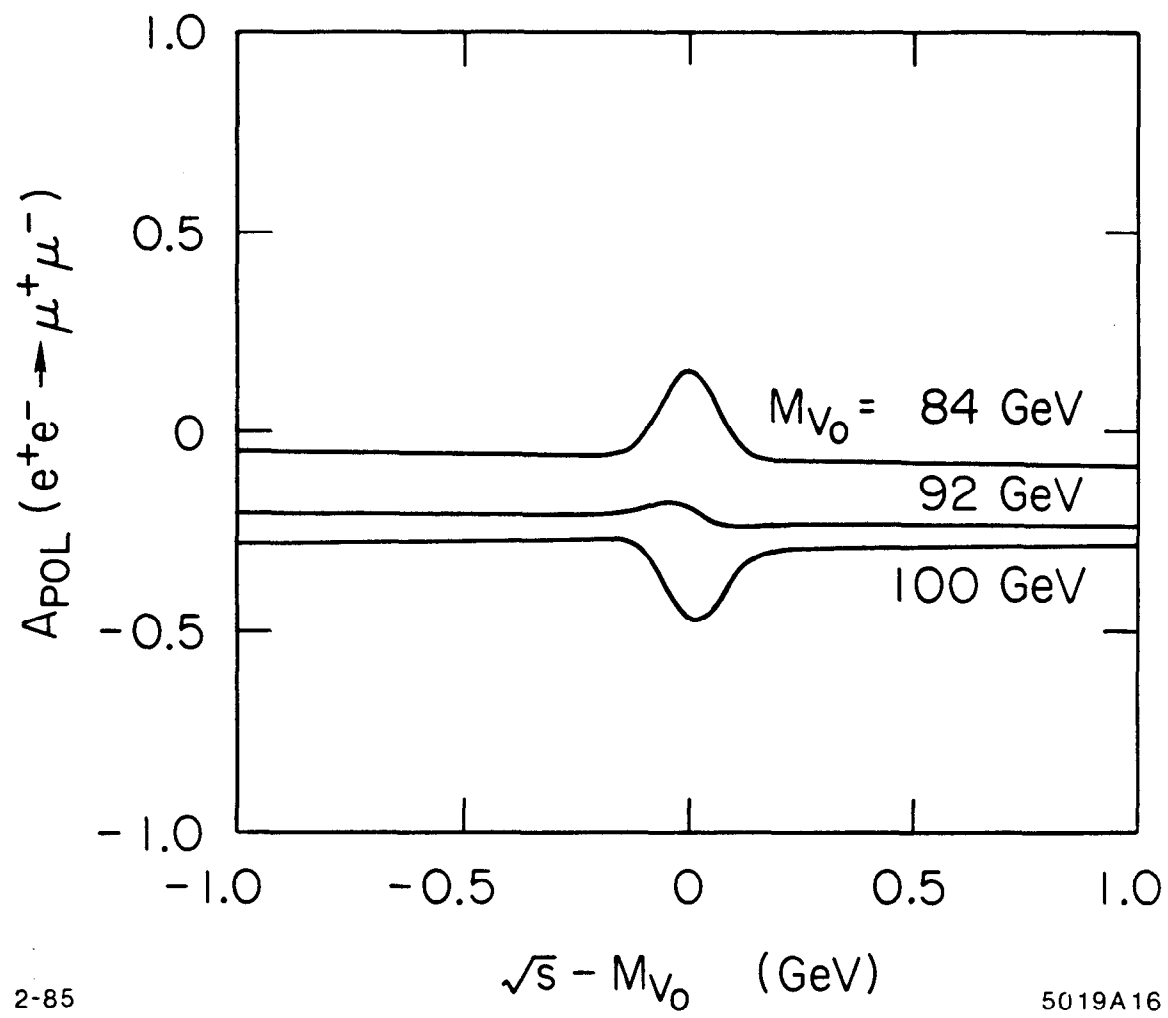
Fig. 13



1-85

5019A11

Fig. 14



2-85

5019A16

Fig. 15

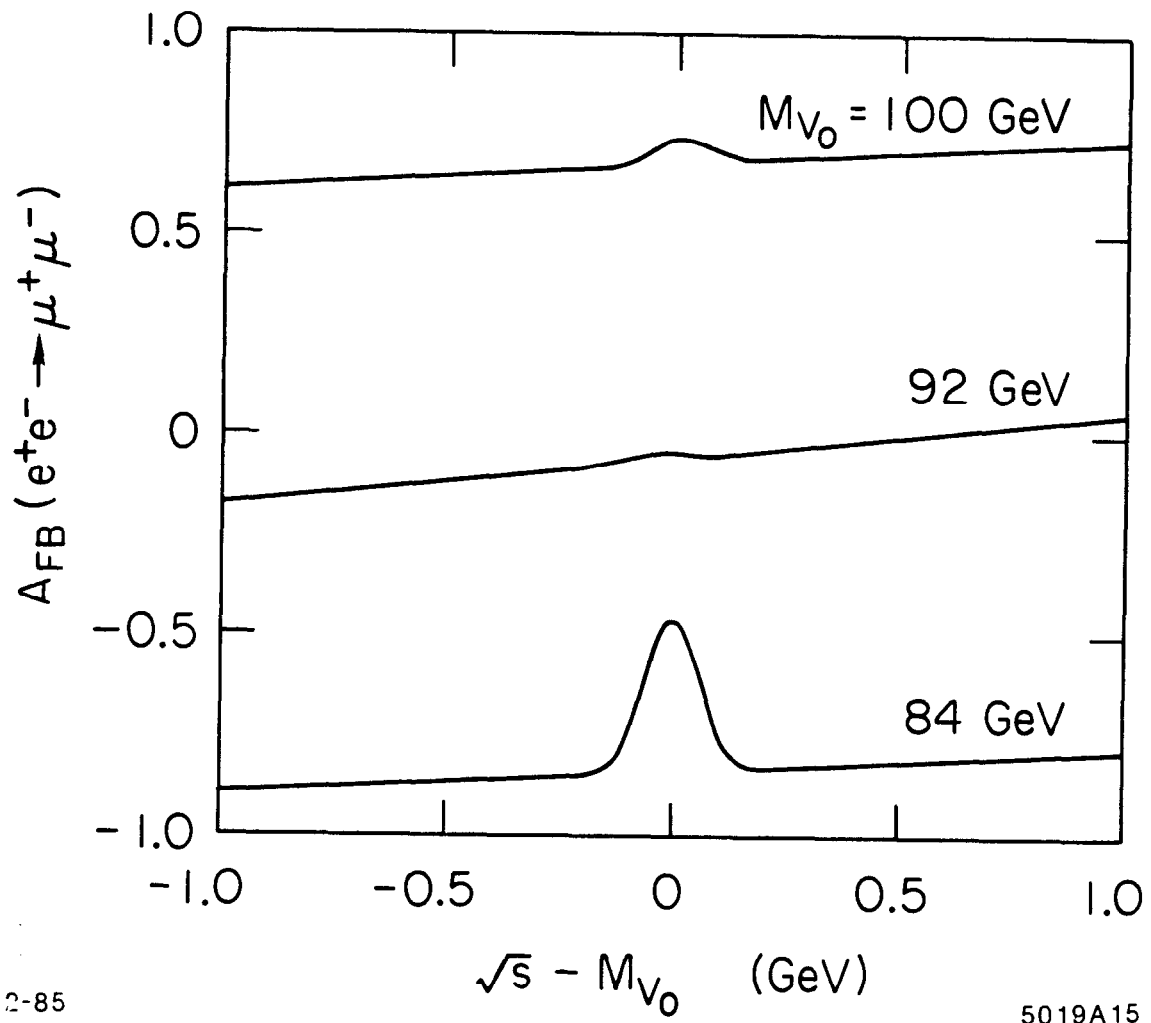


Fig. 16